

Statement of Recent Work - Andrea K. Barreiro

I work in mathematical analysis of neural networks: here, I highlight results on (a) how intrinsic neural dynamics and recurrent coupling impact spike correlation transfer, (b) how we can use easy-to-measure spiking statistics to infer hard-to-measure network features, and (c) how network symmetries affect dynamics in a family of neural networks usually thought of as dominated by “randomness”.

Mechanisms behind correlations in feedforward and recurrent networks

One mechanism behind correlations in neural networks is common input: this is often referred to as *stochastic synchronization*. The simplest example would be a pair of neurons receiving correlated, fluctuating input:

$$I_j = \sigma\sqrt{1-c}\eta_j + \sigma\sqrt{c}\eta_c \quad j = 1, 2 \quad (1)$$

The terms η_j and η_c are independent, fluctuating currents; c regulates the fraction of input that is received by both cells $j = 1, 2$. Each neuron receives the common input, η_c , and therefore their spike trains will be correlated, as quantified by the Pearson’s correlation coefficient between spike counts over a finite time window T , denoted here ρ_T .

In [6, 7], we showed that long-time-window correlations in a *superthreshold* neuron can be well described by using the *phase response curve* (PRC) Z , which quantifies how an input will shift the period of a limit cycle T , depending on the phase θ at which it is received:

$$Z(\theta) = \lim_{\Delta T \rightarrow 0} (T_0 - T_{\Delta T, \theta})/T_0; \quad \lim_{T \rightarrow \infty} \rho_T = cS; \quad S \equiv \frac{\langle Z \rangle^2}{\langle Z^2 \rangle}. \quad (2)$$

The quantity S gives the ratio of the mean of the PRC to its L^2 -norm; thus, it is larger for a Type I neuron (which has Z positive for all values of phase) than a Type II neuron (whose PRC has both positive and negative parts). Because the PRC can be modified experimentally, our results show that ρ_T (or S) is a potential target for neuromodulation.

These asymptotic results were reported in superthreshold neurons in a feedforward network; however, a model for the cerebral cortex would contain *subthreshold* neurons embedded in a *recurrent* network. One widely observed phenomenon is that correlations increase with firing rates: in feedforward networks, this can be explained by the shape of the firing rate-to-input or $f - I$ curve [10]. We studied the relationship between correlations and firing rates in recurrent networks and found that in asynchronous networks typically of cortex models, whether correlations and firing rates covary depends on the mechanisms that underlie firing rate diversity [4]. When the mechanism was variation in intrinsic cell excitability, correlations *did not* increase with firing rate; when the mechanism was variation in mean levels of inhibition, correlations *did* increase with firing rate.

This positive correlation-to-firing rate relationship enhances information in a common population code for motion or orientation direction, which has recently been identified in directionally-sensitive cells in the retina [16, 12]. Therefore, this work outlines a roadmap to determining which network mechanisms can — or cannot — generate a generally beneficial coding structure.

Using neural correlations to probe network structure

As experimental tools advance, measuring whole-brain dynamics with single-neuron resolution is becoming closer to reality [13]. However, a task that remains technically elusive is to measure the interactions within and across brain regions that govern such system-wide dynamics. We recently proposed a procedure to derive constraints on hard-to-measure — such as inter-region synaptic strengths — using easy-to-measure quantities such as firing rates and pairwise correlations [5].

As a test case for our new theoretical tools, we studied interactions in the olfactory system [1]. Our experimental collaborator used two micro-electrode arrays to simultaneously record from

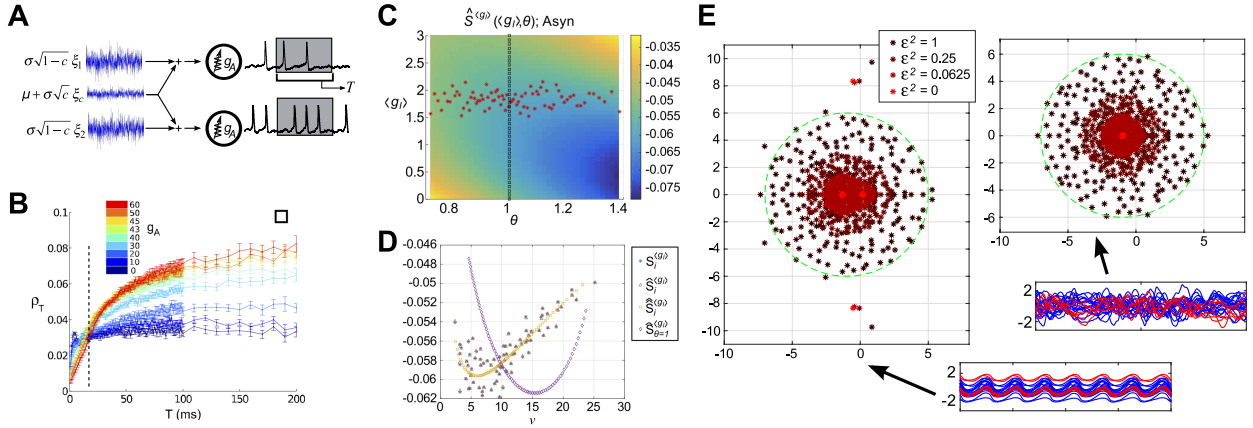


Figure 1: (A) Schematic of two cells receiving common input. (B) The output spike count correlation ρ_T of a pair of Connor-Stevens model neurons (from [7]). (C) Susceptibility to inhibitory conductance fluctuations, $\hat{S}^{(gr)}$, as a function of two intrinsic parameters. (D) Susceptibility as a function of firing rate; depending on how firing rate heterogeneity is achieved, correlations can either increase *or* decrease with firing rate (from [4]). (E) Despite similar spectral behavior, balanced E/I (left) and Gaussian (right) networks show distinctly different trajectories (insets). A subset of excitatory (blue) and inhibitory (red) trajectories from networks of size $N = 200$ are shown (from [3]).

olfactory bulb (**OB**) and anterior piriform cortex (**PC**) of anesthetized rats who were exposed to several odors. We made several predictions about the system, notably that inhibition within OB must be weaker than inhibition within PC. We are currently expanding this method to include higher-order correlations, which can arise in many neural circuits [11, 2].

Low-dimensional dynamics of balanced neural networks

The previous projects analyze spike count correlations in relatively small (and mostly feed-forward) populations; however, realistic neural networks are large and recurrently connected. A common simplification is to consider a network of firing rates (rather than considering individual spikes):

$$\dot{\mathbf{x}} = -\mathbf{x} + \mathbf{G} \tanh(g \mathbf{x})$$

Each cell is either excitatory or inhibitory; thus \mathbf{G} is a matrix with single-signed columns. Also, the network is balanced ($\sum_{j \in E} \mathbf{G}_{ij} + \sum_{j \in I} \mathbf{G}_{ij} \approx 0$) with strong synaptic coupling ($G_{ij} \propto 1/\sqrt{N}$). Such networks are widely used as a theoretical model for cortical dynamics, because they can stably maintain asynchronous firing despite large excitatory and inhibitory currents [14].

We found a novel family of periodic solutions that restrict dynamics to a low-dimensional attractor within a high-dimensional phase space [3]. These solutions arise as a consequence of an underlying symmetry in the mean connectivity structure, and can be predicted and analyzed using equivariant bifurcation theory. We show through concrete examples that these periodic orbits persist in heterogeneous networks, even for large perturbations. These dynamics differ strikingly from the predictions made by random network theory, in a similar setting. This theoretical study provides a possible mechanism to explain experimental studies, in which the input-output functionality of extremely high-dimensional networks has been demonstrated to be encoded dynamically in low-dimensional subspaces [8, 9, 15].

References

- [1] **A.K. Barreiro**, S.H. Gautam, W.L. Shew, and C. Ly. A theoretical framework for analyzing coupled neuronal networks: Application to the olfactory system. Submitted, 2017.
- [2] **A.K. Barreiro**, J. Gjorgjieva, F. Rieke, and E. Shea-Brown. When do microcircuits produce beyond-pairwise correlations? *Frontiers in Computational Neuroscience*, 8, 2014.
- [3] **A.K. Barreiro**, J.N. Kutz, and E. Shlizerman. Symmetries constrain dynamics in a family of balanced neural networks. Submitted (revised): arXiv:1602.05092, 2016.
- [4] **A.K. Barreiro** and C. Ly. When do correlations increase with firing rate? Submitted (revised): arXiv:1610.06598, 2016.
- [5] **A.K. Barreiro** and C. Ly. A practical closure for neural network firing rate models. Submitted, 2017.
- [6] **A.K. Barreiro**, E. Shea-Brown, and E.L. Thilo. Time scales of spike-train correlation for neural oscillators with common drive. *Physical Review E*, 81:011916, 2010.
- [7] **A.K. Barreiro**, E.L. Thilo, and E. Shea-Brown. A-current and type I/type II transition determine collective spiking from common input. *Journal of Neurophysiology*, 108(6):1631–1645, 2012.
- [8] B.M. Broome, V. Jayaraman, and G. Laurent. Encoding and decoding of overlapping odor sequences. *Neuron*, 51(4):467–482, 2006.
- [9] M.M. Churchland, J.P. Cunningham, M.T. Kaufman, J.D. Foster, P. Nuyujukian, S.I. Ryu, and K.V. Shenoy. Neural population dynamics during reaching. *Nature*, 487, 2012.
- [10] J. de la Rocha, B. Doiron, E. Shea-Brown, K. Josić, and A. Reyes. Correlation between neural spike trains increases with firing rate. *Nature*, 448:802–806, 2007.
- [11] A. Fairhall, E. Shea-Brown, and **A.K. Barreiro**. Information theoretic approaches to understanding circuit function. *Current Opinion in Neurobiology*, 22(4):653–659, 2012.
- [12] F. Franke, M. Fiscella, M. Sevelev, B. Roska, A. Hierlemann, and R. Azeredo da Silveira. Structures of neural correlation and how they favor coding. *Neuron*, 89:409–422, 2016.
- [13] R. Prevedel, Y.-G. Yoon, M. Hoffmann, N. Pak, G. Wetzstein, S. Kato, T. Schrödel, R. Raskar, M. Zimmer, E.S. Boyden, and A. Vaziri. Simultaneous whole-animal 3d imaging of neuronal activity using light-field microscopy. *Nat Methods*, 11:727–730, 2014.
- [14] A. Renart, J. de la Rocha, P. Bartho, L. Hollender, N. Parga, A. Reyes, and K.D. Harris. The asynchronous state in cortical circuits. *Science*, 327:587–590, 2010.
- [15] E. Shlizerman, JA Riffell, and JN Kutz. Data-driven inference of network connectivity for modeling the dynamics of neural codes in the insect antennal lobe. *Frontiers in computational neuroscience*, 2014.
- [16] Joel Zylberberg, Jon Cafaro, Maxwell H Turner, Eric Shea-Brown, and Fred Rieke. Direction-selective circuits shape noise to ensure a precise population code. *Neuron*, 89(2):369–383, 2016.